# Diminish the screen effect in field emission via patterned and selective edge growth of ZnO nanorod arrays

Nishuang Liu, Guojia Fang, Wei Zeng, Hao Long, Longyan Yuan et al.

Citation: Appl. Phys. Lett. **95**, 153505 (2009); doi: 10.1063/1.3247887
View online: http://dx.doi.org/10.1063/1.3247887
View Table of Contents: http://apl.aip.org/resource/1/APPLAB/v95/i15
Published by the American Institute of Physics.

# Diminish the screen effect in field emission via patterned and selective edge growth of ZnO nanorod arrays

Nishuang Liu,[1] Guojia Fang,[1,a)] Wei Zeng,[1,2] Hao Long,[1] Longyan Yuan,[1] and Xingzhong Zhao[1]
[1]*Department of Electronic Science and Technology, Key Laboratory of Acoustic and Photonic Materials and Devices of Ministry of Education, School of Physical Science and Technology, Wuhan University, Wuhan 430072, People's Republic of China*
[2]*College of Science, Jiujiang University, Jiujiang 332005, People's Republic of China*

(Received 18 July 2009; accepted 23 September 2009; published online 13 October 2009)

The authors report on the field emission from controlled selective grown zinc oxide (ZnO) nanorod arrays by hydrothermal reaction. With the combined effect from a ZnO seed layer and a passivation layer for nanorod growth, ZnO nanorods could only grow on the edge of a 4 $\mu$m diameter circle. The ZnO nanorods hollow arrays present excellent electron emission characteristics duo to its typical morphology which can significantly diminish the screen effect. By calculating the electrostatic field distribution, it was found that the electrostatic field of the ZnO nanorods hollow arrays is significantly higher than that of the solid arrays. © *2009 American Institute of Physics*. [doi:10.1063/1.3247887]

One-dimensional zinc oxide (ZnO) nanostructures have attracted much attention due to their application to field emission (FE) device.[1] Among the numerous growth methods, the hydrothermally approach[2] is one of the most attractive techniques because it is simple, with low temperature, cost-effective, and easy scalable to large areas. But screen effect is an important factor which depresses the FE performance of the closely packed ZnO nanorods synthesized by hydrothermally approach. Therefore, to diminish the screen effect, a precision control of morphology, alignment, and position are required. Until now, a selective area growth of well-aligned ZnO nanostructures has already been achieved using various techniques such as nanosphere lithography,[3] self-assembled monolayers,[4,5] electron-beam lithography,[6,7] and conventional photolithography.[6] However, these patterning methods, except the conventional photolithography, require expensive masks, complex multistep processes, and costly equipment in some cases. Conventional photolithography is an easy and economical approach to achieve required patterns. But it could only produce micrometer scale pattern, which is absolutely not enough to avoid screen effect in FE. It has been reported that some materials can inhibit the growth of ZnO nanorods, and Qin *et al.*[8] have achieved the laterally aligned growth of ZnO nanowire arrays using the combined effect from ZnO seed layer and these catalytically inactive layer. With this mechanism we can achieve more precision pattern. We just deposited a 50 nm passivation layer on the patterned ZnO seed layer, and found that the quasivertically aligned ZnO nanorods could only grow on the edge of the pattern. The final FE test result has proved that this morphology can significantly diminish the screen effect, which is very important for FE device.

In this paper, we report the selectively controlled growth of submicrometer scale patterned ZnO nanorod arrays on the substrate by a hydrothermally approach. FE properties of ZnO nanorod arrays without patterning and with different patterns were measured and compared. Computer simulation was also utilized for the electrostatic calculation to verify the experimental results.

A (100) silicon (Si) wafer was first cleaned in sequence with HF acid solution, acetone, and ethanol. Before growing the ZnO nanorods, a 300 nm ZnO seed layer was deposited by radio frequency magnetron sputtering. The nutrient solution was an aqueous solution of 0.025*M* zinc nitrate $[Zn(NO3)_2 \cdot 6H_2O]$ and hexamethylenetetramine. The reaction was kept at 90 °C for 2 h. And then we got the ZnO nanorods flat film. To prepare seed layer patterns, a conventional photolithography followed by lift-off techniques was used, and followed by the same growth process. Through this method we can get the ZnO nanorods solid arrays. At last, we sputtered a Sn [or indium tin oxide (ITO)] layer on the patterned ZnO seed layer for preventing the ZnO local growth. After the hydrothermal reaction, we got the ZnO nanorods hollow arrays, which have the best FE performance.

The morphology of the as-grown ZnO nanorods arrays were characterized by FE scanning electron microscopy (FESEM) (FEI XL-30). The FE characteristics were investigated with a two-parallel-plate configuration in a vacuum chamber with a base pressure of $2.0 \times 10^{-5}$ Pa. The cathode area was $1 \times 1$ cm$^2$. The anode and cathode were separated by a 210 $\mu$m Teflon spacer. The current-voltage characteristics were measured by a Keithley 6485 picoammeter and a Keithley 248 high voltage supply.

Figures 1(a) and 1(b) are FESEM images of the ZnO nanorods grown on Si substrates without and with conventional photolithography, which are ZnO nanorod flat film and solid arrays, respectively. As shown in Fig. 1(c), ZnO nanorods of the hollow arrays only grew on the edge of the pattern. From Fig. 1(d), we can observe that ZnO nanorods have a diameter about 200 nm and a length of about 2 $\mu$m. And the hexagonal cross section of nanorods implies that *c* axis of ZnO nanorod is along its length direction. Owing to the covered Sn layer, several ZnO nanorods tilting at various angles to the substrate were grown on the edge of the pattern, as

a)Author to whom correspondence should be addressed. Electronic mail: gjfang@whu.edu.cn.

 

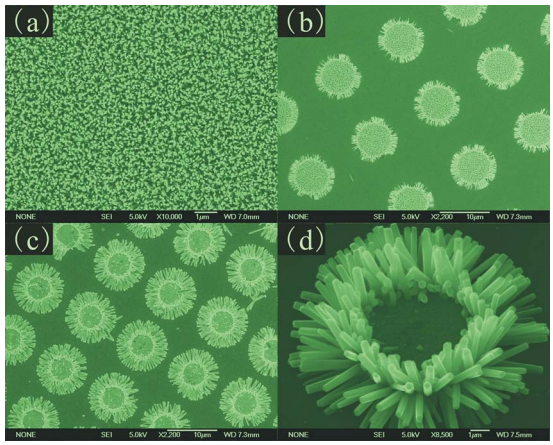


FIG. 1. (Color online) (a) FESEM images of ZnO nanorods flat film, (b) solid arrays, (c) and (d) hollow arrays.

shown in Fig. 1(d). In addition, we can find out that the diameter and length of ZnO nanorods in the hollow arrays are much larger than the flat film and solid arrays. Liu *et al.*[9] believe the consumption of $Zn^{2+}$ may be higher at the area with dense nanorods. Therefore, the growth rate of the high-density nanorods is slower than that at the low-density area.

Generally, Fowler–Nordheim (FN) theory[10] is used to describe FE behavior of metals. The theory is expressed by the following equation:

$$J = A(E^2/\phi)\exp(-B\phi^{3/2}/E),$$

where $J$ is emission current density, $E=\beta E_0$ is the local electrical field, $E_0$ is the mean field between the cathode and anode, $\beta$ is the field enhancement factor, $\phi$ is the work function, and $A$ and $B$ are constants ($A=1.56\times10^{-10}$ A V$^{-2}$ eV $B=6.83\times10^{3}$ V eV$^{-3/2}$ $\mu$m$^{-1}$). The FN plot, $\ln(J/E_0^2)$ versus $1/E_0$, is expected to be a straight line according to the theory.

Figure 2(b) illustrates the FE current density versus electric field characteristics of the three samples shown in Fig. 1. The applied electric field ($E_0$) was defined as $(V\text{-}RI)/D$, where $V$ is the anode voltage, $R$ is resistance of the resistor in series, and $D$ is the cathode-anode distance. To evaluate the FE current density, we simply employ the overall area as emission area. The turn-on field ($E_{to}$) was defined as the electric field at 10 $\mu$A/cm$^2$ of $J$. As shown in the figure, the ZnO nanorods flat film performed poorly as a field emitter, which is generally attributed to a screening effect.[7,9,11] And the solid arrays showed a relative better FE characteristic. The FE data reveal that the hollow arrays showed the best FE performance. It turned on at an electric field of 4.4 V/$\mu$m, and the threshold field ($E_{th}$), where $J$ reaches 1 mA/cm$^2$ was 5.56 V/$\mu$m. As displayed in the inset of Fig. 2(a),

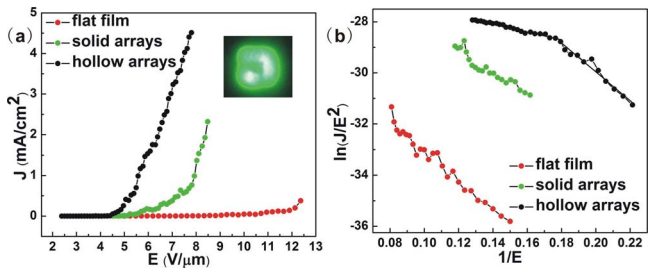


FIG. 2. (Color online) (a) FE current density vs electric field plot for the ZnO nanorods flat film, solid arrays and hollow arrays. (b) The FN plots of the field emission $J$-$E$ characteristic curves.

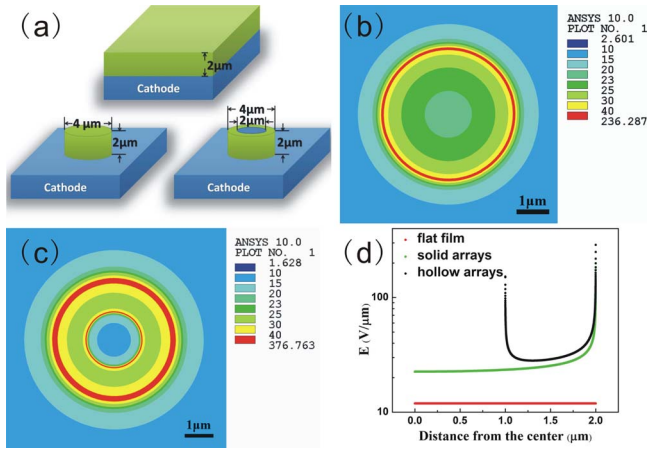


FIG. 3. (Color online) (a) Models for simulation of electrostatic potential. Top down views of simulated electric-field distributions for (b) column and (c) cylinder. (d) Calculated electric-field distributions of all these samples ranged from the center axis to outer side of one circular unit.

the brightness of the hollow arrays is relative uniform. As shown in Fig. 2(b), a two-slope behavior is observed in the FN curves for the hollow arrays, while no such change is observed in the other two samples. Such two-slope characteristics are also reported in many other types of field emitters. However, the mechanism of the multistage slope phenomena is not clear yet, there are many suppose to explain these phenomena, such as energy band, adsorbates, and defects.[12,13] In general, for ZnO nanostructure, slope shows a small value at a low applied voltage and a large value at a high voltage. However, in the present case, what we observed is just opposite to the reports about ZnO mentioned above. In fact, this two-slope behavior is similar to the FE from carbon nanotube (CNT), which is considered to originate in a saturation of the emission current caused by space charge effect.[14] Considering the fact that all our samples were produced by the same method, it can't be these characters such as energy band, adsorbates or defects that contribute to this two-slope behavior. The difference between our samples is probably due to differences in the emission sites. A larger number of emission sites prevent the saturation of the emission current at higher applied voltage. This is because the larger number of emission sites reduces the emission current per one ZnO nanorod on the sample under comparison at the same current density.

To investigate the origin of the efficient FE from the hollow arrays, we simulated the electrostatic field based on the finite element method with ANSYS v10.0 software. Because the as-grown ZnO nanorods are so much dense as bulk material, we just used flat film, column, and cylinder as the models to make the simulation simple, as shown in Fig. 3(a). For investigating the trends of variation of electric field on the top surfaces of simples, three paths are established from the center axis to outer side radially in the model. An anode to cathode separation of 210 $\mu$m was used, and a positive potential of 2500 V was applied to the anode. The as simulated electric-field distributions of ZnO column and cylinder are shown as a top down view in Figs. 3(b) and 3(c). It can be clearly seen that the electric field of the cylinder is significantly higher than the column. In addition, Fig. 3(d) shows the simulated electric-field distributions of all these samples ranged from the center axis to outer side. It was found that the electric field of the column is significantly

TABLE I. Key performance parameters of some ZnO nanorods field emitters reported in the literature about diminishing the screen effect and this work.

| Manufacture technique | Turn-on field ($V/\mu m$) | Threshold field ($V/\mu m$) | Reference |
|---|---|---|---|
| Electron-beam lithography | 2.85at 10 $\mu A/cm^2$ | 3.2 at0.052 $mA/cm^2$ | 6 |
| Electron-beam lithography | 0.13at0.1 $\mu A/cm^2$ | 9 at 1 $mA/cm^2$ | 7 |
| Density control via layer-by-layer polymer | 5.1 at 10 $\mu A/cm^2$ | 7 at 50 $\mu A/cm^2$ | 11 |
| Density control via ultrathin seed layer | 7.1 at 10 $\mu A/cm^2$ | 10 at 1 $mA/cm^2$ | 9 |
| Nanorods hollow arrays | 4.4 at 10 $\mu A/cm^2$ | 5.56at 1 $mA/cm^2$ | This work |

higher at the edge (162 $V/\mu m$) than that at the center (22 $V/\mu m$), whereas the electric field of the flat film is constant all over the emitter surface. We can find that the electric field of the cylinder is also significantly higher at the edge (152 $V/\mu m$ at the inner edge and 290 $V/\mu m$ at the outer edge), and it is higher than electric field of the column all over the range. These results imply that the electric field is predominantly concentrated in ZnO nanorods at the edge of the array. Therefore, the highly efficient FE of the hollow arrays can be attributed to the reduction of screen effect.

Until now, there are already many reports about diminishing the screen effect of the ZnO nanorods synthesized by hydrothermally approach. For comparison, Table I tabulates the manufacture techniques and key performance parameters of the ZnO field emitters reported in the literature and this work. As shown in the table, our sample is better than most of them, except the first one from Ref. 6. But considering the expense and difficulty of technique, we believe our solution is obviously an effective way to diminish the screen effect. Besides comparing with ZnO nanorods synthesized by hydrothermally approach, the emission characteristics of the as-grown ZnO nanorods are comparable with a majority of inorganic semiconductor nanostructures and CNT.[15–19]

In conclusion, our controlled selective growth of ZnO nanorods arrays provides a way to fabricate high-performance electron emitters at a low temperature of 90 °C. With the combined effect from a ZnO seed layer and the passivation layer, we can fabricate quasivertically aligned ZnO nanorods on the edge of a 4 $\mu m$ diameter circle. The ZnO nanorod hollow arrays had excellent FE characteristics, which were due to the diminishing of screen effect from the typical morphology. By calculating the electrostatic field distribution, it was found that the electrostatic field of the ZnO nanorod hollow arrays was significantly higher than the solid arrays. Our results imply that ZnO nanorods synthesized by hydrothermally approach are promising candidates for vacuum electronic-device application.

This work was supported by the Special Fund of Ministry of Education for Doctor's Conferment Post (Grant No. 20070486015) and the National High Technology Research and Development Program of China (Grant No. 2009AA03Z219).

[1] N. S. Xu and S. E. Huq, Mater. Sci. Eng. R. **48**, 47 (2005).
[2] Q. Ahsanulhaq, A. Umar, and Y. B. Hahn, Nanotechnology **18**, 115603 (2007).
[3] H. J. Fan, B. Fuhrmann, R. Scholz, F. Syrowatka, A. Dadgar, A. Krost, and M. Zacharias, J. Cryst. Growth **287**, 34 (2006).
[4] D. F. Liu, Y. J. Xiang, X. C. Wu, Z. X. Zhang, L. F. Liu, L. Song, X. W. Zhao, S. D. Luo, W. J. Ma, J. Shen, W. Y. Zhou, G. Wang, C. Y. Wang, and S. S. Xie, Nano Lett. **6**, 2375 (2006).
[5] Y. Masuda, N. Kinoshita, F. Sato, and K. Koumoto, Cryst. Growth Des. **6**, 75 (2006).
[6] A. Ahsanulhaq, J. H. Kim, and Y. B. Hahn, Nanotechnology **18**, 485307 (2007).
[7] Y. J. Kim, J. Yoo, B. H. Kwon, Y. J. Hong, C. H. Lee, and G. C. Yi, Nanotechnology **19**, 315202 (2008).
[8] Y. Qin, R. S. Yang, and Z. L. Wang, J. Phys. Chem. C **112**, 18734 (2008).
[9] J. Liu, J. She, S. Deng, J. Chen, and N. S. Xu, J. Phys. Chem. C **112**, 11685 (2008).
[10] R. H. Fowler and L. Nordheim, Proc. R. Soc. London, Ser. A **119**, 173 (1928).
[11] B. Weintraub, S. Chang, S. Singamaneni, W. Han, Y. Choi, J. Bae, M. Kirkham, V. V. Tsukruk, and Y. Deng, Nanotechnology **19**, 435302 (2008).
[12] N. S. Ramgir, D. J. Late, A. B. Bhise, I. S. Mulla, M. A. More, D. S. Joag, and V. K. Pillai, Nanotechnology **17**, 2730 (2006).
[13] C. X. Xu, X. W. Sun, S. N. Fang, X. H. Yang, M. B. Yu, G. P. Zhu, and Y. P. Cui, Appl. Phys. Lett. **88**, 161921 (2006).
[14] Y. C. Choi, Y. M. Shin, D. J. Bae, S. C. Lim, Y. H. Lee, and B. S. Lee, Diamond Relat. Mater. **10**, 1457 (2001).
[15] X. S. Fang, Y. Bando, U. K. Gautam, C. Ye, and D. Golberg, J. Mater. Chem. **18**, 509 (2008).
[16] X. S. Fang, Y. Bando, G. Shen, C. Ye, U. K. Gautam, P. M. F. J. Costa, C. Zhi, C. Tang, and D. Golberg, Adv. Mater. **19**, 2593 (2007).
[17] J. Liu, Z. Zhang, Y. Zhao, X. Su, S. Liu, and E. Wang, Small **1**, 310 (2005).
[18] X. S. Fang, Y. Bando, C. Ye, G. Shen, U. K. Gautam, C. Tang, and D. Golberg, Chem. Commun. (Cambridge) **2007**, 40.
[19] S. S. Fan, M. G. Chapline, N. R. Franklin, T. W. Tombler, A. M. Cassell, and H. Dai, Science **283**, 512 (1999).